

Multiple melting behavior of a thermotropic copolyester containing spirobicycromane moiety

Lieh-Li Lin^a, Jin-Long Hong^{b,*}

^aDepartment of Chemical Engineering, Chengshiu Institute of Technology, Kaohsiung 83342, Taiwan, ROC

^bInstitute of Materials Science and Engineering, National Sun Yat-Sen University, Kaohsiung 80424, Taiwan, ROC

Received 9 November 1999; received in revised form 4 January 2000; accepted 1 February 2000

Abstract

A thermotropic copolyester I-19 prepared from a rigid, bent spirobicycromane (SPI), 1,7-heptanediol (HD), and an aromatic ester triad, TOBC (terephthaloyl bis(4-oxybenzoyl chloride), was prepared and its thermal behavior investigated by differential scanning calorimetry. Copolyester I-19 exhibited completely different DSC thermograms between samples cooled from the isotropic liquid and the mesomorphic states, a result attributable to the registry effect of the neighboring chains in the mesophase. Non-isothermal crystallization at different cooling/heating rates, and isothermal crystallization and annealing at various temperatures had been conducted to verify the origins of the complicated four melting endotherms (as T_{m1} , T_{m2} , T_{m3} and T_{m4} from high- to low-temperature regions) in the sample cooled from the mesomorphic state. The highest-temperature T_{m1} transition is attributed to the melting of the primary crystal formed via the liquid crystalline nuclei. T_{m2} and T_{m3} transitions are due to melting of the less perfect, secondary crystals close and less close to the pure crystals responsible for the T_{m1} transition. By choosing suitable isothermal crystallization and annealing processes, T_{m2} and T_{m3} transitions can be moved to merge with T_{m1} to become one high-temperature single melting endotherm. The lowest-temperature T_{m4} transition, which basically remained intact after different thermal treatments, is caused by the melting of the chain segments near the SPI moieties. © 2000 Elsevier Science Ltd. All rights reserved.

Keywords: Thermotropic copolyester; Multiple melting

1. Introduction

Many papers had been published in the last decade dealing with the crystallization behavior of a number of thermotropic polyesters. In cases of nematic copolyesters with fully aromatic rigid backbones, phenomena such as the absence of massive structural rearrangements [1] and negligible volume change during nematic to solid states [2] had been observed. To describe the crystallization kinetics of the fully aromatic copolyesters prepared from 1,4-dihydroxybenzoic acid (HBA) and 2,6-dihydroxynaphthoic acid (HNA), [3–6] a two transition processes referred to the fast solidification and a slow crystal transition steps had been suggested. Study on this system revealed that the fast process during quenching from nematic melts forms crystals with hexagonal packing while the slow process, [4] which develops in the remaining parts of the samples, constructs crystals with orthorhombic packing. The two transition processes can

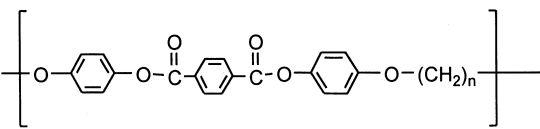
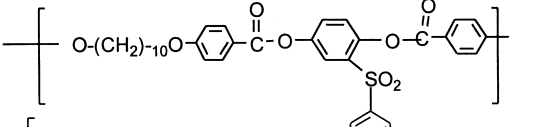
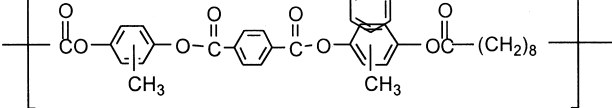
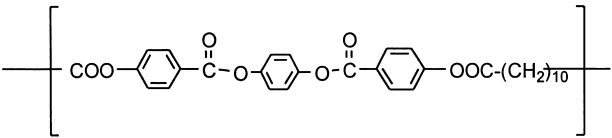
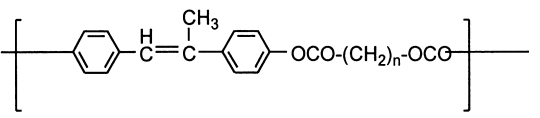
justify the results reported on HTR polymer (copolymer prepared from terephthalic acid, phenylhydroquinone, and phenylether hydroquinone), [6] even in this case some differences arising have been attributed to a solid-state post-polymerization, simultaneously present with crystal perfection.

The chain structure regularity and molecular motion should have profound influence on the crystallization behavior of thermotropic polyesters. In contrast to the fully aromatic copolyesters, complicated results had been reported for the crystallization behavior of the semi-rigid thermotropic polyesters [7–12]. Chemical structures of the respective polyesters and the origins of the multiple melting behaviors were summarized in Table 1. The multiple melting transitions on DSC analysis of polyesters, PO, [7] prepared from different aliphatic diols and an aromatic mesogenic triad were attributed to the possible polymorphism existing in the samples. A main chain thermotropic polyester, PSHQ10, [8] was subjected to DSC investigations at different heating rates. Conclusion based on the resulting DSC thermograms suggested that the high-temperature melting crystals originated from the recrystallization and

* Corresponding author. Tel.: + 886-7525-2000, ext. 4065; fax: + 886-7-525-4099.

E-mail address: jlhong@mail.nsysu.edu.tw (J.-L. Hong).

Table 1
Chemical structures of different semi-rigid polyesters and the origins for their multiple melting behaviors

Chemical structure	Symbol	Origin for multiple melting
	PO	Polymorphism
	PSHQ10	Recrystallization and perfection
	PM1	Registry of neighboring chains in the nematic state
	PM2	Registry of neighboring chains in the nematic state
	HMS-n	Registry of neighboring chains in the nematic state

perfection of the crystals during isothermal annealing. In comparison to the two mechanisms mentioned above, chain registry [10–12] in the nematic state had also been presented to account for the melting and crystallization behavior of different semi-rigid polyesters (as PM1, PM2 and HMS-n listed in Table 1). This hypothesis described that certain registry of neighboring chains in the nematic state can serve as potential nuclei for primary crystal and the crystals formed in the remaining portions upon secondary crystallization. This theory was indirectly proved by different thermal treatments in the isotropic and nematic states.

All the semi-rigid thermotropic polyesters described above possess nematic mesophase and a double melting endotherms during DSC scans. In our laboratory, we had prepared a semi-rigid, thermotropic copolyester system (Fig. 1) from polycondensation reactions between TOBC (terephthaloyl bis(4-oxobenzoyl chloride) and HD (1,7-heptanediol), and SPI (spirobicyclic) diols [13]. Among those copolyesters we synthesized, copolyester I-19 (the inherent SPI moiety is 10 mol%) exhibited interesting multiple melting behavior (cf. Fig. 2d–f) under DSC scan. Here, use of spiro SPI monomer is due to its rigid, bent geometry imposed by the central quaternary carbon and its steric bulkiness (cf. the simulated structure in the up-right corner of Fig. 1). Aligned chain packing around the SPI-rich segments would be conceivably difficult in considering the bent structure of SPI units. Therefore, SPI content in the corresponding copolyester has decisive effect on the liquid

crystalline properties; that is, no more mesomorphism was resulted for copolyester with a SPI content higher than 20 mol%.

Previously, spiro SPI moieties had been incorporated in polyamides, polyimides, and polyesters [14–18]. Among them, aromatic polyesters and copolyesters [18] prepared from a combined monomers of 3-(4-hydroxyphenyl)-1,1,3-trimethyl-5-indanol, bisphenol A, isophthaloyl and terephthaloyl chloride were amorphous and readily soluble in common organic solvents. This example may illustrate the detrimental effect of the spiro compounds on polymer crystallinity. Similarly, we expected that the bent and bulky SPI unit should disrupt the chain alignment in the mesomorphic state once it was built into thermotropic polymers. Here, HD and TOBC monomers were chosen to polymerize with SPI since polyester prepared from HD and TOBC possesses low thermal transitions ($T_m = 176^\circ\text{C}$, $T_i = 253^\circ\text{C}$) and wide mesomorphic range ($\Delta T = 77^\circ\text{C}$); [19] therefore, copolyester I-19 thus synthesized has its melting transitions at temperatures below 200°C and thermal treatments can be performed safely at low temperatures without the potential interference from solid-state polymerization [6] occurred at high temperatures. This unexpected reaction may obscure the interpretations for the already complicated multiple melting behavior for I-19. In addition, copolyester I-19 distinguishes it from other semi-rigid polyester systems by a more ordered smectic, instead of nematic, mesophase as revealed by our WAXD study. The more ordered smectic mesophase for copolyester I-19 may have stronger chain

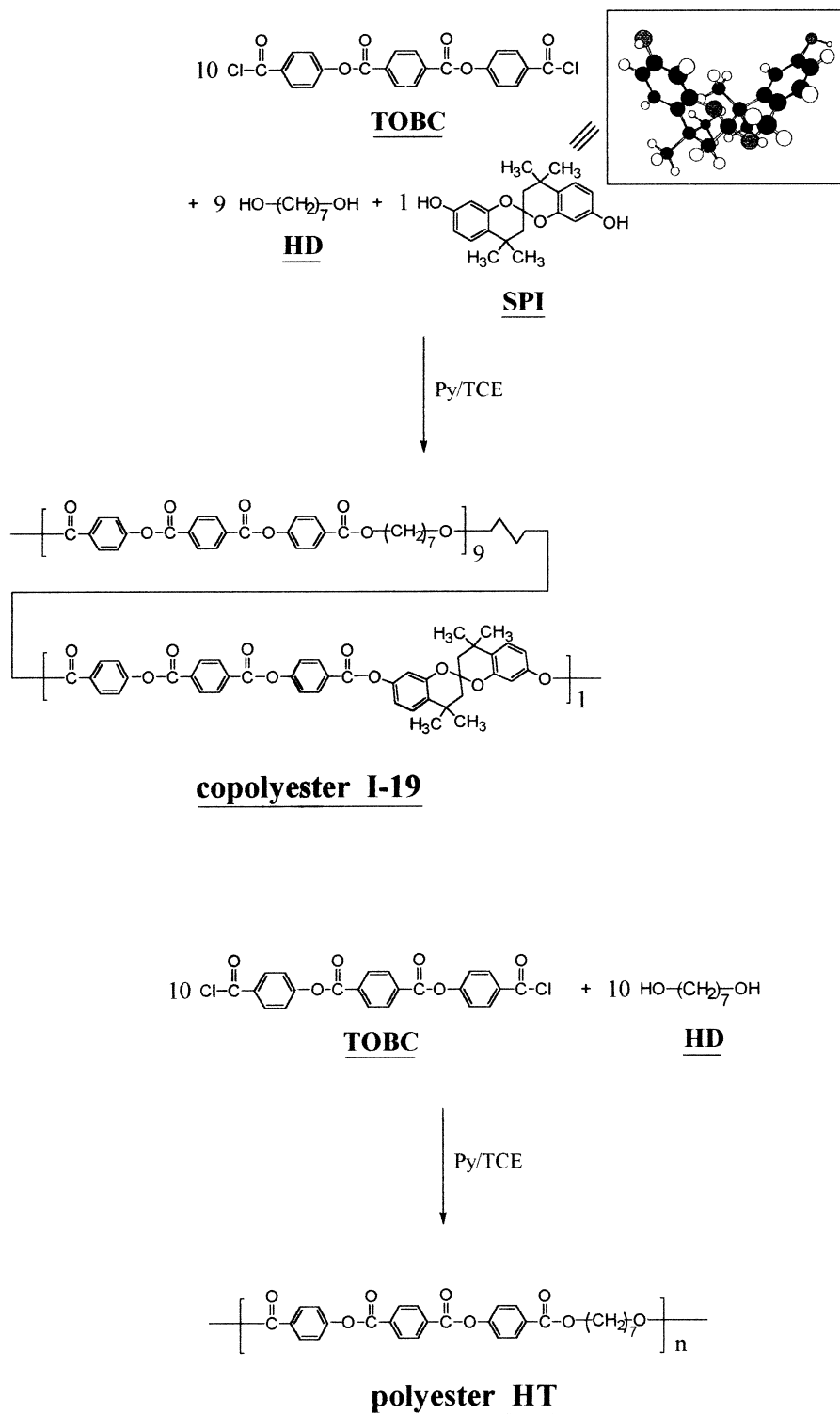


Fig. 1. Syntheses of copolyester I-19 and homopolyester HT (simulated structure of spirobicyclic mannequin (SPI) was also included).

registry effect as compared with other nematic polyesters as listed in Table 1.

In this study, non-isothermal crystallizations at different heating/cooling rates and isothermal crystallization at various temperatures were conducted to clarify the origins of the four melting endotherms observed for copolyester I-

19. Wide-angle X-ray diffraction (WAXD) study on samples subjected to different thermal treatments was also carried out to evaluate the effect of thermal history on crystal structures. In addition, homopolyester HT (cf. Fig. 1 for the chemical structure) was also prepared from polycondensation reaction of TOBC and HD, and used as a model

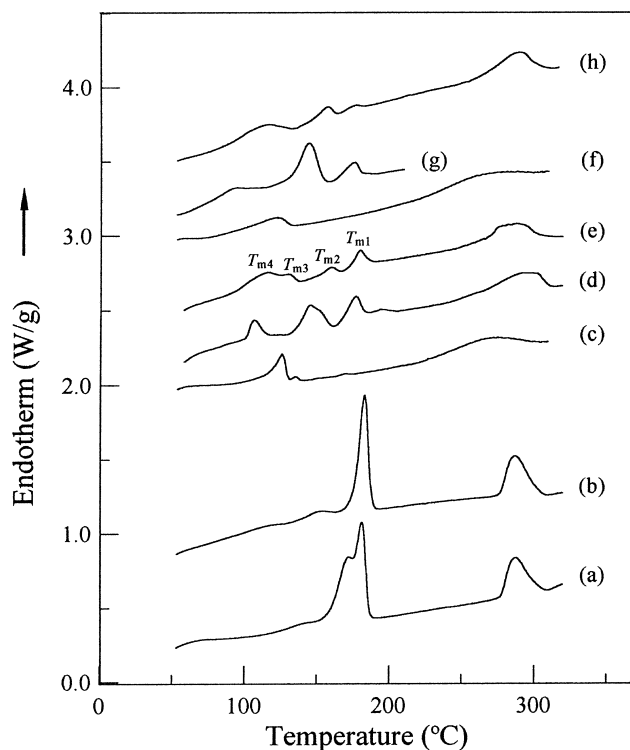


Fig. 2. DSC thermograms of: (a) the as-synthesized HT; (b) the as-synthesized HT after heating at 210°C for 3 min; (c) the as-synthesized HT after heating to 310°C; and (d) the as-synthesized copolyester I-19; (e) the as-synthesized copolyester I-19 after heating at 210°C for 3 min; (f) the as-synthesized copolyester I-19 after heating to 310°C; (g) copolyester I-19 after heated to 310°C, and re-dissolved in TCE before vacuum drying; and (h) re-heating run after scan (g). (the cooling rate after the respective thermal treatments and the heating rate for all thermograms are 20°C/min).

polymer to compare with copolyester I-19 in terms of thermal properties and WAXD result. Finally, we provide a scheme to rationalize the possible mechanisms for the formation of the multiple melting behavior.

2. Experimental section

2.1. Materials

Terephthaloyl chloride and *p*-hydroxybenzoic acid were recrystallized from hexane and distilled water, respectively. Pyridine was distilled after dehydration with KOH. 1,7-Heptanediol was vacuum dried at 50°C for 12 h and stored over molecular sieve 4 Å (Linde). 1,1,2,2-Tetrachloroethane (TCE) was pre-dried over molecular sieve 4 Å (Linde) for at least one week before use. Spirobicromane (SPI, Tokyo Chem. Inc., >99%) and thionyl chloride (Ferak, 99%) were used directly without purification. Polyester HT and copolyester I-19 were synthesized according to the procedures described previously [13].

2.2. Instrumental analysis

Inherent viscosity of copolyester I-19 ($\eta_{inh} = 0.31$ dl/g)

was measured at a concentration of 0.5 g/dl in TCE, using a Ubbelohde viscometer at 30°C. Inherent viscosity of polyester HT can not be measured due to its insolubility in common organic solvent. The liquid crystalline texture was observed with a Nikon Optiphot-POL microscope equipped with a Linkam TMS controller and THMS 600 hot stage.

Thermal transition temperatures were detected with a Perkin-Elmer DSC-7 model. The carrier gas was nitrogen at a flow rate of ca. 10 ml/min, and sample pans were always filled with approximately the same quantity of 6 mg of sample. Calibration of the calorimeter was conducted for each heating rate using with indium and lead standards. The as-synthesized sample was heated to either the smectic or the isotropic liquid states before further thermal treatments. Pre-treatment in the smectic state was performed by heating the sample at 210°C for 3 min; it has been observed that reproducible results were obtained by changing the time at 210°C from 3 to 30 min. This temperature is higher than the extrapolated metastable equilibrium melting temperature (= 185°C) derived, as described by Cheng, [3] on the basis of the relationship between melting temperature and crystallization time at different temperatures. Pre-treatment in the isotropic liquid state was performed by heating sample to 310°C before cooling (cooling rate = 20°C/min) immediately to the desired temperature for further thermal process. Different thermal processes for samples cooled from the mesomorphic state were described as following:

The non-isothermal crystallization samples were cooled (cooling rate = 20°C/min) from 210°C at different rates (5, 10, and 20°C/min) before re-heating to obtain the DSC thermograms.

The isothermal crystallization samples were quenched (cooling rate = 200°C/min) from 210°C to the crystallization temperatures (T_{cs} , ranging from 105 to 160°C) and kept there for different time periods (t_c). The samples were then cooled (cooling rate = 20°C/min) to room temperature and re-heated to obtain the DSC traces. In two runs (at $T_{cs} = 135$ and 155°C), re-heating experiments were performed right after the isothermal crystallization process, and the immediate re-scan of the DSC traces recorded. Peak temperatures for the heating cycle were used. T_{m1} , T_{m2} , T_{m3} , and T_{m4} correspond to the positions of the first, second, third, and fourth endothermic peaks from the high to low temperature portions.

In the annealing experiments, samples were heated at 210°C for 3 min, cooled with a rate of 20°C/min to room temperature, and then heated to the chosen annealing temperature (T_a , ranging from 80 to 165°C), and kept there for different times (t_a). The samples were again cooled at a rate of 20°C/min to room temperature before re-heating to yield the DSC thermograms.

WAXD experiments were carried out at room temperature with a Siemens Diffraktometer D 5000 model (CuK α Ni-filtered radiation). Specimens subjected to different annealing processes were used.

3. Results and discussion

3.1. Primary characterizations on polyester HT and copolyester I-19

Synthesis of copolyester I-19 were performed according to Fig. 1. Similarly, homopolyester HT was prepared from direct polycondensation between TOBC and HD. For copolyester I-19, mixture of monomeric HD and SPI diols in a molar ratio of 9 to 1 were added slowly to a solution of TOBC in TCE solvent. Due to the reactivity difference between HD and SPI toward TOBC monomer, the resulting copolyester I-19 may have a comonomer sequence distribution of more “blocky” nature, a comment had been addressed in our previous contribution [13]. Previous study also evaluated that both HT and I-19 polymers possess a smectic C_2 type of mesophase, [20–22] in which the mesogenic units in each layer are tilted to the layer normal but with their tilt direction apposite to each other between neighboring layers.

Homopolyester HT was firstly investigated by DSC. The as-synthesized HT exhibited a shoulder-like transition before the major double-melting endotherms in the temperature ranges of 150–190°C and the T_i transition at 288°C (Fig. 2a). If the first scan of the as-synthesized HT sample was stopped at the mesomorphic state (210°C) for 3 min, the subsequent re-heating run resulted in a thermogram (Fig. 2b) consisting of a major melting endotherm at ~180°C and a T_i transition with its shape and position similar with the one in the as-synthesized sample (Fig. 2a). Suggestively, different crystalline structures induced by the TCE solvent used in the synthesis step can be varied by thermal treatment. Alternatively, if the as-synthesized HT was heated to the isotropic liquid state (310°C), the subsequent DSC thermogram after cooling would exhibit a completely different feature (Fig. 2c) with the T_m transition appeared with less intensity and at lower temperature ranges as compared with the as-synthesized one (cf. Fig. 2a).

Similar thermal treatments were also performed on copolyester I-19. The as-synthesized copolyester I-19 exhibited complicated multiple melting transitions (T_m s) in the temperature ranges of 100–200°C before the final isotropization transition (T_i) centered at 288°C (Fig. 2d). The as-synthesized copolyester I-19 after heated at 210°C for 3 min exhibited a DSC thermograms (Fig. 2e) of multiple melting endotherms, which are significantly different from the as-synthesized one (cf. Fig. 2d). The second and the third rescans all resulted in the same DSC thermogram as Fig. 2e as long as the heating was secured at temperatures below T_i . In contrast, thermal treatment of copolyester I-19 at temperature (= 310°C) higher than T_i resulted in a thermogram (Fig. 2f) with only one broad low-temperature T_m , and one broad T_i transition at lower temperatures than the as-synthesized sample. The sample after heated to the isotropic liquid state has similar DSC thermogram despite further thermal treatment at 210°C for any time period up to 3 h.

Here, we may argue that the possible transesterification reaction (or decomposition) during heating at 310°C may be the cause for the difference between Fig. 2e and f. The possibility of major transesterification (or decomposition) during isotropization process can be excluded by further experiment; that is, copolyester I-19 after pre-heated at 310°C was re-dissolved in TCE to erase the thermal history of the treated polymer. The resulting sample after precipitation and drying was further scanned in DSC to result in a thermogram of multiple melting endotherms (Fig. 2g), whose global features are different from those in the as-synthesized sample (cf. Fig. 2d). Second rescan of this solvent-treated sample after cooled from 210°C yielded a thermogram (Fig. 2h), which is slightly different from those in Fig. 2e. Preservation of the multiple melting behavior for the solvent-treated sample suggests that no major transesterification (or decomposition) reaction occurred during short-time stay at 310°C. Slight difference between the solvent-treated (Fig. 2h) and the second rescan after cooled from 210°C (Fig. 2e) may be an indication of minor decomposition. However, this minor decomposition should not be responsible for the major discrepancy between Fig. 2e and f.

As suggested above, both copolyester I-19 and polyester HT exhibited different DSC traces between the samples cooled from the isotropic liquid and the mesomorphic states. Presumably, the previous thermal history determines the thermal behavior of the corresponding samples. Sample cooled from the ordered mesomorphic state preserves the ordered mesomorphic chain arrangement, which will serve as the primary nuclei for the subsequent crystallization according to the hypothesis of chain registry [10–12] in the mesomorphic state. In contrast, sample after heated to the isotropic liquid state (referred to as the isotropically randomized sample) would lose the ordered mesomorphic chain arrangement, which is difficult to resume by additional thermal treatments. Suggestively, the capability of the isotropically randomized sample to resume its original mesomorphic order is strongly influence by its chain geometry effect in the mesophase. This is especially true for copolyester I-19 since its inherent rigid, bent SPI moieties would efficiently prevent the polymeric chains to pack into an ordered arrangement from the isotropically randomized state. Separate results in our laboratory had suggested that the capability from the isotropically randomized to the original mesomorphic states is governed by the chain flexibility (or chemical structure) of the corresponding polymers, a subject will be discussed in our next publication and will not be detailed here.

The multiple melting behavior for the sample cooled from 210°C (cf. Fig. 2e) is determined by the chain arrangement in the previous smectic C_2 state. The three low-melting transitions, labeled as T_{m2} , T_{m3} (as a broad left-shoulder to T_{m4}), and T_{m4} , are broad in shape, and the high-melting T_{m1} appears at a position close to the melting transition of HT homopolyester (cf. Fig. 2a or b); therefore, melting of pure $-(H-T)-$ domain may be

Table 2
Adapted data from the non-isothermal crystallization DSC runs

Heating rate (°C/min)	Cooling rate (°C/min)	T_{m4} (°C)	T_{m3} (°C)	T_{m2} (°C)	T_{m1} (°C)	$\Delta H_{\text{m4}}^{\text{a}}$ (J/g)	$\Delta H_{\text{m3}}^{\text{b}}$ (J/g)	$\Delta H_{\text{m2}}^{\text{a}}$ (J/g)	$\Delta H_{\text{m1}}^{\text{b}}$ (J/g)	$\Delta H_{\text{total}}^{\text{c}}$ (J/g)
20	20	115.0	130.5	157.2	177.2	7.76	0.86	1.08	2.02	11.72
	10	115.0	131.1	157.2	177.2	6.90	0.16	1.98	2.74	11.78
	5	109.7	— ^d	157.2	177.2	4.12	— ^d	3.56	3.82	11.50
10	20	113.8	130.5	157.2	177.2	7.50	0.66	1.02	3.68	12.86
	10	115.4	131.2	157.2	177.2	6.76	0.28	1.72	4.90	13.66
	5	107.8	— ^d	157.2	177.2	4.88	— ^d	3.30	5.32	13.50
5	20	114.2	130.9	157.2	177.2	8.86	1.20	0.80	7.82	18.68
	10	115.1	131.8	157.2	177.2	7.50	0.48	1.56	8.34	17.88
	5	111.8	— ^d	157.2	177.2	5.18	— ^d	2.52	8.42	16.12

^a Enthalpy was evaluated by two times the heat involved between the on-set and peak temperatures.

^b Enthalpy was evaluated by two times the heat involved between the peak and ending temperatures.

^c Total enthalpies involved in T_{m1} , T_{m2} , T_{m3} and T_{m4} transitions.

^d No T_{m3} was observed in this case.

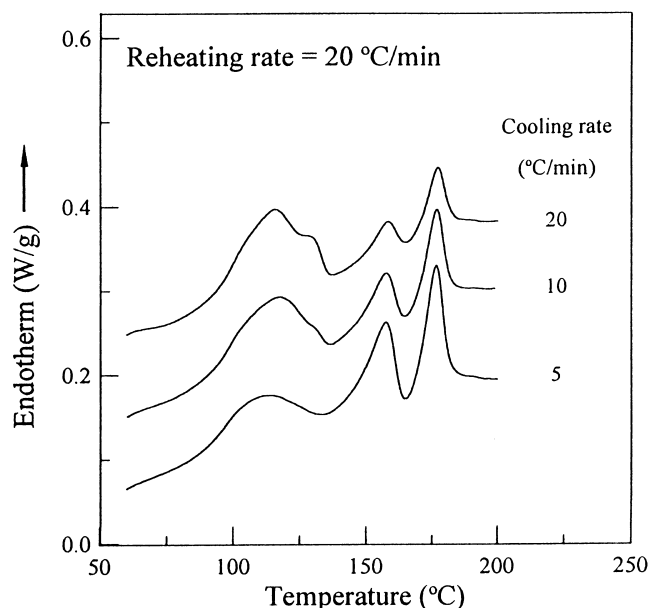


Fig. 3. Non-isothermal crystallization DSC scans of copolyester I-19 at a reheating rates of 20°C/min after cooling from 210°C at different rates.

responsible for this high-temperature T_{m1} transition. With the reproducible thermograms, we thereafter conducted different experiments to evaluate the inter-relationship between these four melting endotherms in the copolyester I-19 after cooled from 210°C.

3.2. Multiple melting behavior of copolyester I-19

Samples that have been non-isothermally crystallized were re-heated at constant rate of 20, 10 and 5°C/min and selected DSC thermogram with a heating rate of 20°C are shown in Fig. 3. Under different non-isothermal crystallization conditions, the higher melting T_{m1} and T_{m2} transitions remain at the same positions. In contrast, the shoulder-like transition, T_{m3} , exhibited a strong dependence on cooling rate, that is, it is absent in sample cooled with a slow rate of 5°C/min but becomes significant in sample cooled with a rate of 20°C/min. The observation reflects the instability of the crystal representing T_{m3} transition. In all cases, the lowest T_{m4} transition is broad in shape and in-separate with the small T_{m3} transition. Small exothermic heats were observed in all thermograms with a pre-cooling rate of 5°C/min, and became more significant if a lower re-heating rate was applied.

Peak temperature and enthalpy adapted from all DSC runs were summarized in Table 2. The influence of the heating/cooling rate on the peak position is limited for the low-temperature T_{m3} and T_{m4} transitions; as for the high-temperature T_{m1} and T_{m2} transitions, they remained intact with their peak temperatures kept at 177.2 and 157.2°C, respectively. General trend on the resolved enthalpy can be commented if we overlooked the small exothermic heat between T_{m1} and T_{m2} in certain cases. With a constant

heating rate, enthalpies of the high-temperature T_{m1} and T_{m2} increased at the expense of enthalpies involved in the low-temperature region (T_{m3} and T_{m4}). Total enthalpies (ΔH_{total}) depend strongly on the heating rate, and are increased with a slow heating rate. Suggestively, crystal structures are enhanced with a lower heating rate, and this is especially true for the high-temperature T_{m1} and T_{m2} transitions. It seems that the pre-cooling rate effect little on ΔH_{total} , a phenomenon possibly associated to the strong memory effect of the corresponding mesomorphic state and will be discussed later.

The multiple-melting behavior has previously attributed to reasons including the presence of different crystal structure, [23–25] or to crystal reorganization, [26–29] or to different components of the morphology formed in two stage of crystallization [30,31]. The presence of different crystal structure can lead to multiple-melting peak in the DSC thermogram, but will be excluded from the X-ray diffraction pattern described latter.

When crystal reorganization during heating occurs, the lower melting point and the size of the higher one are strongly dependent on heating rates. As the heating rate increases, the reorganized portion decreases, and this results in a reduction of the higher endotherm and an increase of the lower one, which shifts towards higher temperatures. Since the lower melting point is correlated to the original crystals present, it strongly depends on the crystallization conditions and therefore, in non-isothermal crystallization process, on the cooling rate. The lower the cooling rate, the larger is the time available for crystals to form a more perfect structure and so they exhibit a higher melting point. Therefore, multiple melting peaks originating from reorganization process should have their peak temperatures dependent on the cooling and heating rates. The relatively constant peak temperatures under different non-isothermal conditions suggest that, at least, reorganization mechanism can not account for the interrelationship between these four melting transitions. The decreasing enthalpies of the high-temperature T_{m1} and T_{m2} transitions with increasing heating rate also can be used to account for the above comment. To continually evaluate the complicated relationship between these four melting transitions, careful isothermal crystallization experiments at selected temperature (T_c) were further conducted.

Samples isothermally crystallized between 105 and 160°C showed different heating traces dependent on the crystallization time (t_c). In all processes, ultimate t_c of 120 min was used since prolonged crystallization caused no change on the resulting thermograms. Selected DSC scans after isothermally crystallized at 105 and 120°C were shown in Fig. 4a and b, respectively. Both figures have similar feature that the high-temperature T_{m1} and T_{m2} transitions remained intact while the low-temperature T_{m3} and T_{m4} varied their peak temperatures and intensities with t_c . For T_{m3} transition, the peak gained its intensity during the process; in contrast, the T_{m4} transition gradually lost its intensity and shifted to lower temperatures with time. Variation on

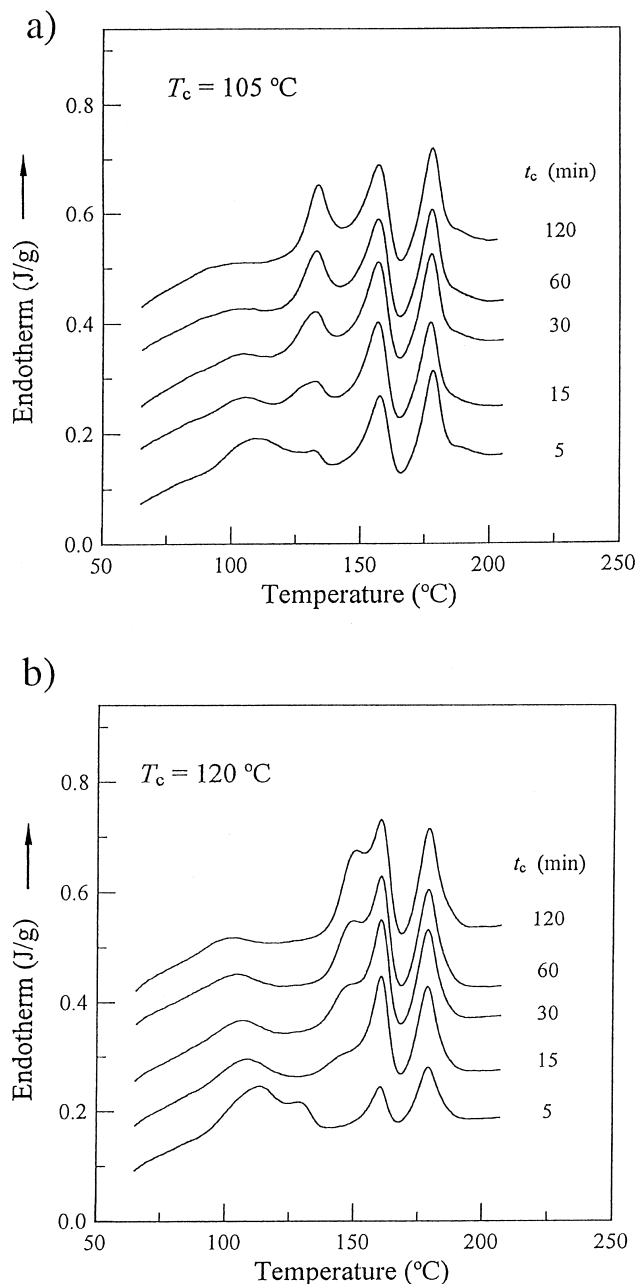


Fig. 4. DSC thermograms of copolyester I-19 after isothermal crystallization at: (a) 105; and (b) 120°C for various time.

the high-temperature regions is more significant for case of T_c at 120°C (Fig. 4b); here, we observed the obvious enlargements of the T_{m1} and T_{m2} transition from $t_c = 5$ to 15 min. Concurrently, T_{m3} transition was shifted upward to meet the high-temperature T_{m2} , and continually increased its intensity during the process.

DSC thermograms of samples after treated at $T_c > 135^\circ\text{C}$ for 120 min were summarized in Fig. 5. At $T_c = 135^\circ\text{C}$, T_{m3} transition finally combined with T_{m2} to become one single broad peak. Samples crystallized at 135, 140, and 145°C basically have similar thermograms; however, T_{m2} transition gradually shifted to higher temperature to overlap with T_{m1}

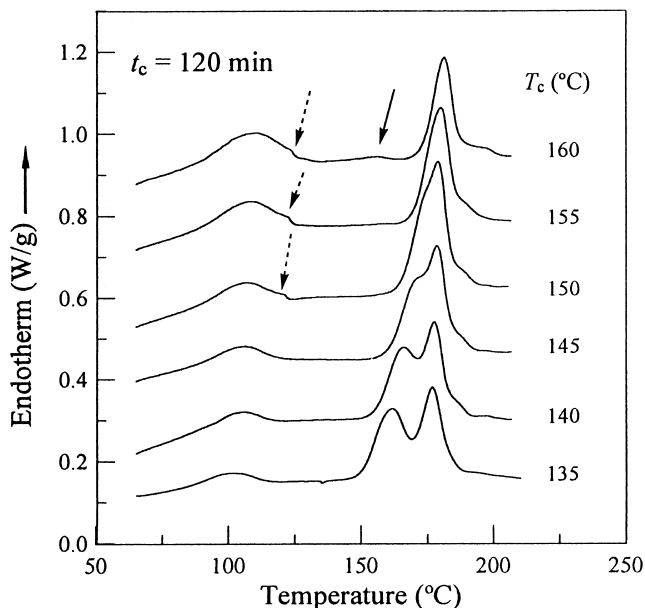
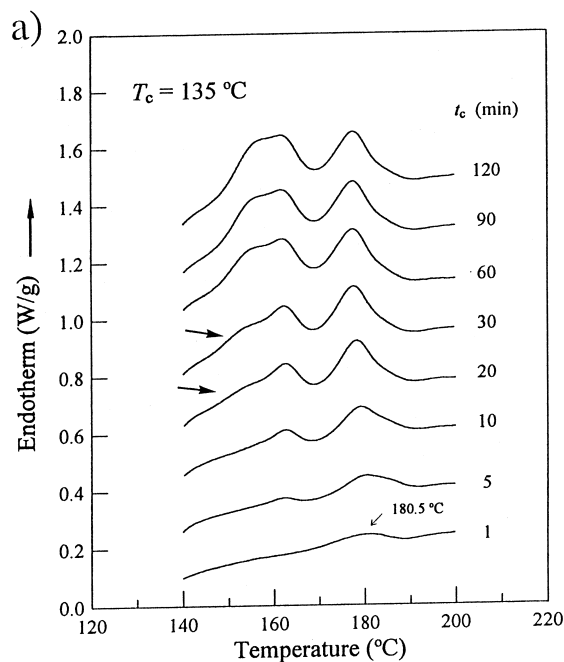


Fig. 5. DSC thermograms of copolyester I-19 after isothermal crystallization at different temperatures for 120 min (heating rate = 20°C/min).

transition as T_c is increased. In case of $T_c = 150^\circ\text{C}$, T_{m2} transition finally merged with T_{m1} to become one single, unsymmetrical peak. Samples after isothermally crystallized at 155 and 160°C possessed a DSC thermograms with only one single high-temperature T_{m1} transition. Comparatively, DSC thermograms of samples crystallized at a higher T_c of 160°C exhibited a T_{m1} transition of less intensities than those from $T_c = 155^\circ\text{C}$ and a small endotherm (as indicated by arrow) originated from recrystallization of certain molten chains during cooling stage was also visualized. Certain imperfect crystals formed during isothermal crystallization at a higher T_c will be situated in the molten state if a higher T_c was applied; this corresponds to the lower intensity of T_{m1} transition in case of $T_c = 160^\circ\text{C}$ as compared with $T_c = 155^\circ\text{C}$. All DSC thermograms in Fig. 5 showed the progressive increase of the low-temperature T_{m4} transition with increasing T_c . Small tiny transitions (as indicated by dashed arrows) located approximately in the temperature ranges of T_{m3} transition were observed in cases of $T_{cs} = 150, 155,$ and 160°C . Formations of less perfect crystals representing the low-temperature T_{m3} and T_{m4} transitions are more significant for samples cooled from a higher T_{cs} .

Samples isothermally crystallized can be rescanned immediately to clarify the relationship between the high-melting T_{m1} and T_{m2} transitions. The immediate rescan after crystallization at 135°C (Fig. 6a) showed that T_{m1} transition formed early at $t_c = 1$ min before the first appearance of T_{m2} transition at $t_c = 5$ min. Peak intensity of T_{m1} increased from $t_c = 1$ to 60 min and remained relatively constant thereafter; on the contrary, T_{m2} transition continually changed its shape and intensity through the whole crystallization process. The above observations suggests



b)

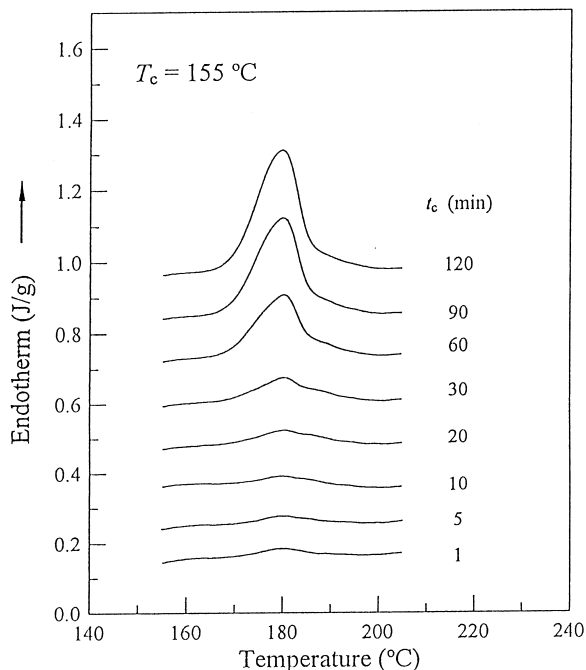


Fig. 6. Immediate rescans of copolyester I-19 after crystallization at: (a) 135; and (b) 155°C for various time (heating rate = 20°C/min).

that T_{m1} is not generated from the reorganization of the T_{m2} transition. Here, the shoulder-like endotherm developed in the low-temperature region (as indicated by the arrows) may be the T_{m3} transition coming from the low-temperature region, a process observed in the isothermal crystallization experiment, too (cf. Fig. 5a). The immediate rescan after crystallized at 155°C (Fig. 6b) showed only one melting endotherm centered at a slightly higher temperature of

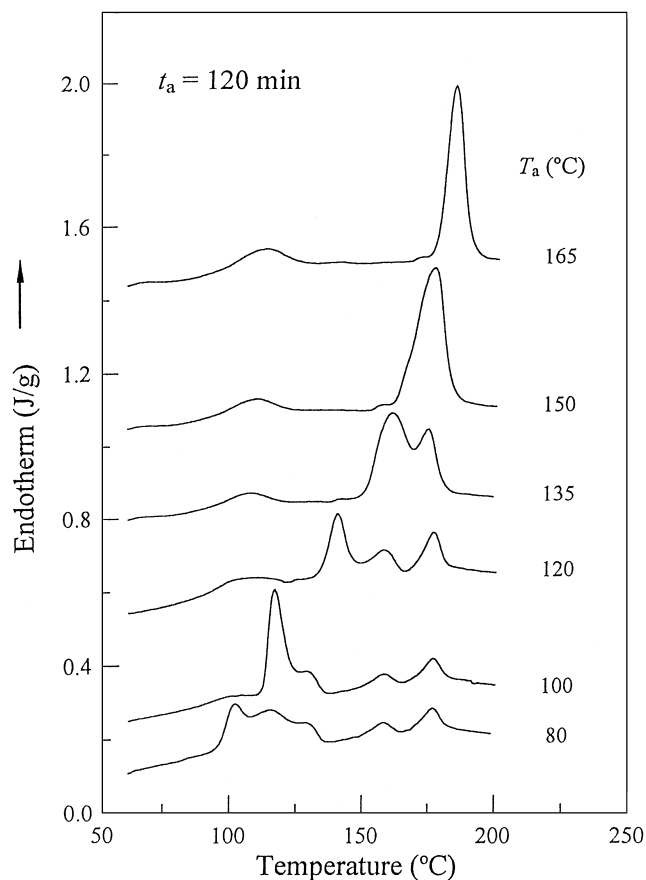


Fig. 7. DSC thermograms of copolyester I-19 after annealing at different temperatures (T_a s) for 120 min (heating rate = 20°C/min).

180°C as compared to that crystallized at 135°C (in this case, T_{m1} peak was centered at 177°C). The high endothermic enthalpy (11.83 J/g at $t_c = 120$ min) suggests the crystals corresponding to the T_{m1} transition easily formed at a higher T_c of 155°C.

Samples annealed at different temperatures (T_a s), ranging between 80 and 165°C, were subjected to DSC scans to reveal the origins of the multiple melting behavior for copolyester I-19. Samples annealed at each temperature had their DSC traces dependent on the annealing time (for each T_a , five t_a s of 0, 5, 30, 60 and 120 min were applied). For the sake of simplicity, only the results from $t_a = 120$ min were illustrated in Fig. 7, in which all the DSC traces showed one particularly intense melting endotherm centered at ~20°C higher than the T_a s used in the annealing procedures. For samples annealed at 80°C, a large endotherm besides the T_{m1} , T_{m2} , T_{m3} and T_{m4} transitions was observed. This result may suggest the prevalence of the solid-state crystallization for copolyester I-19. Samples annealed at temperatures >120°C all resulted in a thermograms with their low-temperature T_{m4} s appearing at the same temperature ranges, indicating the unique nature of this imperfect crystals representing the T_{m4} transition. Samples annealed at 150 and 165°C exhibited only one single high-temperature melting peak with the respective melting enthalpy higher than that

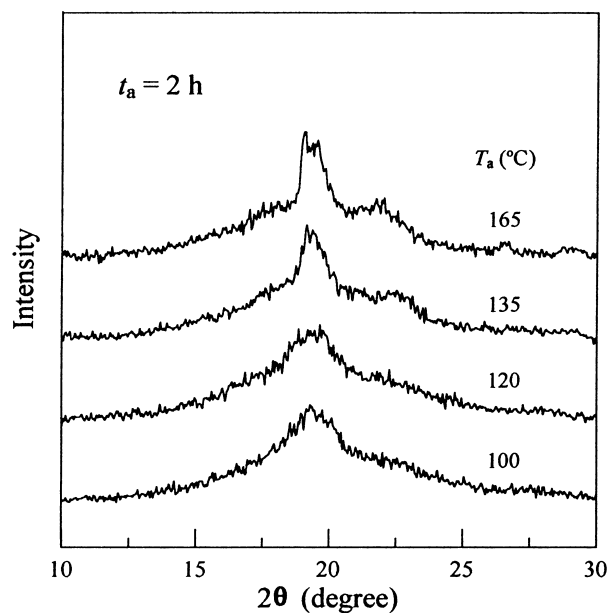


Fig. 8. X-ray diffractograms of copolyester I-19 after annealing at different temperatures for 2 h.

obtained from the isothermal crystallization experiments. Here, we clearly observed only two transitions representing the T_{m1} and T_{m4} transitions, a result indicating that the four melting transitions are not due to the heterogeneous molecular weight distribution in the as-synthesized I-19. The resulting two transition peaks may suggest the existence of two segment units distributed along the polymer chain.

In order to clarify the origin of the multiple endotherm, X-ray study had been carried out on samples suitably treated such that their DSC traces exhibited different multiple melting peaks varied with annealing temperatures for 2h (the corresponding DSC thermograms were shown in Fig. 7). X-ray diffraction patterns of copolyester I-19 after annealing at 100–165°C were shown in Fig. 8. The smooth variations on the wide-angle diffraction patterns with crystallization time may reflect certain crystal perfection process, but besides that, no new diffraction peak formed during the annealing process. Similar X-ray study performed on samples after different isothermal crystallization experiments also caused no formation of new diffraction peak and will not present here. Therefore, the different thermal behaviors cannot be ascribed to the presence of different crystal structures.

As described in Section 1, multiple melting behavior had been previously [7–12] discovered in several semi-rigid thermotropic polyesters and attributed to different mechanisms. Study on poly[(phenylsulfonyl)-*p*-phenylene-1,10-decamethylenbis(4-oxybenzoate)] (PSHQ10) [8] suggests that its high-temperature melting crystals were originated from the recrystallization and perfection process. The involvement of major reorganization process between T_{m1} , T_{m2} and T_{m2} , T_{m3} transition pairs can be excluded from isothermal immediate rescan and

non-isothermal crystallization experiments. The reverse trend of T_{m4} and T_{m3} transition temperatures toward T_c s also violates the principle of reorganization process. Other studies [10–12] on semi-rigid thermotropic polyesters revealed that their multiple melting behavior depends strongly on the preliminary thermal history on the mesomorphic state. It is said that, due to the slow evolution of the mesomorphic melt towards its thermodynamic equilibrium, a certain registry of neighboring chains persists in the melt. This persistent registry can be regarded as potential nuclei of the rigid chains arising from nematic melt is related to the low melting endotherm.

The role of SPI in copolyester I-19 can be viewed in two aspects, i.e. its possible sequence distribution and its influence on the neighboring chains. Copolyester was prepared by polycondensation of TOBC with mixed diols of SPI and HD (cf. Fig. 1). Previously, Ignatious et al. [32] had suggested that phenolic hydroxyl groups have higher reactivity than alcoholic hydroxyls towards terephthaloyl chloride. Therefore, during synthesis of copolyester I-19, the aromatic SPI would react preferentially and be incorporated into the oligomeric chains formed early in the reaction in higher proportion than its initial mole fraction in the comonomer mixture. The less reactive HD monomer may participate in the copolymerization to an increasing extent as the concentration of the more reactive SPI monomer was depleted by the preferential reaction. Therefore, despite its limited amounts (10 wt%) of SPI monomer used in the synthesis step, the resulting copolyester I-19 may contain sequence of the same $-(S-P)-$ repeat units, i.e. they have certain SPI-rich domains.

Understanding the possible block nature of copolyester I-19, the potential effect of SPI moieties on neighboring chains can be then emphasized. Despite its limited amount of concentrations of SPI moieties in the chain, its effect on chain arrangements in the mesomorphic states may be drastic. The bent geometry of SPI moieties would impose a non-linear chain arrangement on the neighboring mesogenic triads, and prevent formation of an ordered, parallel chain arrangement required for smectic layer structure. The effect may be long range since a bent structure, once formed, it would take several neighboring $-(H-T)-$ chain segments to readjust before reaching an ordered smectic layers of considerable dimensions. The detrimental effect of SPI on chain packing is more significant if we studied copolyester (as copolyester I-28) sample with 20 mol% of SPI moiety. With more content of SPI units, copolyester exhibited an unidentified mesomorphic texture (X-ray diffraction peaks appear at the same positions as copolyester I-19 does) with its average domain size comparatively smaller than this copolyester I-19. In addition, DSC thermogram of copolyester cooled from 210°C showed only a broad T_m ($\sim 100^\circ\text{C}$) and T_i ($\sim 277^\circ\text{C}$) appeared at relatively lower position than copolyester I-19. No mesomorphism can be detected for copolyester sample with 40 mol% of SPI moieties. This experimental result suggests the detrimental effect of SPI units on mesomorphic order.

It is then suggested that different $-(H-T)-$ domains may have their size and perfection varied dependent on their distances from the destructive SPI moieties. Variation on the domain size in addition to the potential chain registry in the smectic C mesophase all contributed to the complicated multiple melting behavior for copolyester I-19. To explain the crystallization behavior, a certain registry of neighboring chains persisting in the smectic C_2 state is taken into account. The registry of neighboring chain is supposed to become poorer and poorer and finally disappear when equilibrium state is attained. Here, we are not dealing with conventional nuclei of crystallization; in fact, the temperature (210°C) chosen to treat the samples in the smectic state is high enough to prevent this possibility. According to the procedures reported by Cheng, [3] we can extrapolate the metastable equilibrium melting temperature ($= 185^\circ\text{C}$), which appears to be lower than 210°C. We can therefore consider the persistent registry of neighboring chains as potential nuclei of crystallization, responsible for certain melting peaks of copolyester I-19.

In considering the detrimental effect of the SPI moieties in copolyester I-19, crystallization of the $-(H-T)-$ segments should depend strongly on their relative distance from the SPI-moieties. Cooling from the ordered smectic C state, the persistent registry of neighboring chains resulted in the formation of primary crystals, responsible for the high-temperature T_{m1} , and the low-temperature T_{m4} transitions. The primary crystals responsible for the T_{m1} transition may be thicker, more perfect, higher melting, and reside in the pure $-(H-T)-$ domains; in contrast, the low-temperature T_{m4} transition may be due to the imperfect crystals, which are $-(H-T)-$ segments near the SPI moieties. Within the remaining portions, secondary crystallization takes place to form crystals of thinner, less perfect and lower melting than crystals representing T_{m1} . Under subsequent heating cycle, these crystals were melt to give two endotherms, T_{m2} and T_{m3} . The high-temperature T_{m2} peak may be attributed to the melting of secondary crystals close to the pure $-(H-T)-$ domain. In contrast, in region less close to the pure $-(H-T)-$ domains, secondary crystals formed, and melt to give T_{m3} peak during heating. By isothermal crystallization between 130 and 140°C, chain segments can be moved to match neighboring chains by a slight translation motion, resulting in the thickening and perfection process and the merge of T_{m2} and T_{m3} transitions as observed in DSC thermograms of Fig. 5a and b. Similarly, subsequent chain matching further proceeded and resulted in the formation of a large, high-melting pure $-(H-T)-$ domain. It is proposed here that the merge of transitions T_{m2} , T_{m3} , and then T_{m1} transitions all corresponds to movements of chain segments remote from the SPI moieties. In contrast, the primary crystal of the $-(H-T)-$ chain segments near the SPI moieties are relatively inert to all thermal treatment due to the neighboring rigid, aromatic $-(S-T)-$ segments. This resulted in the basically similar feature of T_{m4} transition under annealing at temperatures higher than 120°C (Fig. 7)

4. Conclusion

Both polyester HT and copolyester I-19 showed distinguished DSC thermograms dependent on its previous thermal history. Upon heated to the corresponding isotropic liquid states, both polymers possess a low-temperature melting endotherm; in contrast, samples cooled from the ordered smectic C phase exhibited multiple melting endotherms in both the low- and high-temperature regions. The registry of the neighboring chains in the mesomorphic state is supposed to play a determining role on the melting behavior under subsequent heating scans. Upon heated to the isotropic liquid state, chain arrangements of both polyesters were randomized and can not be completely resumed by further thermal treatments.

Upon cooled from the mesomorphic state, copolyester I-19 exhibited a complicated four melting transitions of T_{m1} , T_{m2} , T_{m3} and T_{m4} as counting from the high-temperature region. T_{m1} transition corresponds to melting of primary crystal of pure $-(H-T)-$ domain while T_{m4} , is due to the melting of $-(H-T)-$ segments near the SPI moieties. The transitions in the middle temperature ranges, T_{m2} and T_{m3} , come from the secondary crystals formed during cooling from the mesomorphic state. Secondary crystals close to the pure $-(H-T)-$ domain are responsible for the T_{m2} transition while those less close to the pure $-(H-T)-$ domain melt to form T_{m3} transition. Both T_{m2} and T_{m3} transitions can be thermally treated to merge with the high-temperature T_{m1} transition.

Acknowledgements

We appreciate the financial support of the National Science Council, R.O.C., under contract no. NSC-88-2216-E-110-005.

References

- [1] Warner SB, Jaffe M. *J Cryst Growth* 1980;48:184.

- [2] Bechtoldt H, Wendorff JH, Zimmermann H. *J Makromol Chem* 1987;188:651.
- [3] Cheng SZD. *Macromolecules* 1988;21:2475.
- [4] Cheng SZD, Janimak JJ, Zhang A, Zhou Z. *Macromolecules* 1989;22:4240.
- [5] Butzbach GD, Wendorff JH, Zimmermann H. *J Polym* 1986;27:1337.
- [6] Ghanem AM, Dickinson LC, Porter RS, Zachariades AE. *J Polym Sci, Polym Phys Ed* 1990;28:1891.
- [7] Antoun S, Lenz RW, Jin J-I. *J Polym Sci, Polym Chem Ed* 1981;19:1901.
- [8] Han CD, Chang S, Kim SS. *Macromolecules* 1994;27:7699.
- [9] Marsano E, Salati U, Valenti B. *Polymer* 1993;34:1232.
- [10] Carpaneto L, Marsano E, Valenti B, Zanardi G. *Polymer* 1992;33:3865.
- [11] Carpaneto L, Marsano E, Salati U, Valenti B. *Polymer* 1993;34:3464.
- [12] Cheng Y-Y, Cebe P, Capel M, Schreuder-Gibson H, Bluhm A, Yeomans W. *J Polym Sci, Polym Phys Ed* 1995;33:2331.
- [13] Lin LL, Hong JL. *Polymer* 2000;41:2419.
- [14] Wilson JC. *J Polym Sci, Polym Chem Ed* 1975;13:749.
- [15] Hsiao SH, Yang CY. *J Polym Sci, Polym Chem Ed* 1997;35:1479.
- [16] Hsiao SH, Yang CP, Yang CY. *J Polym Sci, Polym Chem Ed* 1997;35:1487.
- [17] Schmidhauser JC, Longley KL. *Polym Prepr* 1989;30(1):13.
- [18] Imai Y, Tassavori S. *J Polym Sci, Polym Chem Ed* 1984;22:1319.
- [19] Ober C, Jin J-I, Lenz RW. *Polym J* 1982;14:9.
- [20] Ellis G, Lorente J, Marco C, Gomez MA, Fatou JG, Hendra P. *J. Spectrochim. Acta* 1991;47A:1353.
- [21] Watanabe J, Hayashi M. *Macromolecules* 1989;22:4083.
- [22] Brand HR, Cladis PE, Pleiner H. *Macromolecules* 1992;25:7223.
- [23] Lovering EG, Wooden DC. *J Polym Sci, Polym Phys Ed* 1969;7:1639.
- [24] Samuel RS. *J Polym Sci, Polym Phys Ed* 1975;13:1417.
- [25] Prest Jr. WM, Luca DJ. *J Appl Phys* 1975;46:1136.
- [26] Alfonso GC, Pedemonte E, Ponzetti L. *Polymer* 1979;20:104.
- [27] Lemstra PJ, Kosistra T, Challa G. *J Polym Sci, Polym Phys Ed* 1972;10:823.
- [28] Mandelkern L, Allow AL. *J Polym Sci, Polym Lett Ed* 1966;4:447.
- [29] Lee Y, Porter SR, Lin JS. *Macromolecules* 1989;22:1756.
- [30] Butzbach GD, Wendorff JH, Zimmermann H. *J Polym* 1986;27:1337.
- [31] Basset DC, Olley RH, Al Raheil IAM. *Polymer* 1988;29:1745.
- [32] Ignatious F, Lu C, Kantor SW, Lenz RW. *Macromolecules* 1994;27:7785.